



15th Canadian Masonry Symposium
Ottawa, Canada
June 2-5, 2025



Numerical Analysis of Infill Wall Interaction with Frames

Daniel Quiunⁱ and Qenti Herenciaⁱⁱ

ABSTRACT

Many buildings with reinforced concrete (RC) frames have infill walls. In Peru, the common masonry units used in such walls are horizontally-hollow or perforated clay bricks. An experimental program was done in 2016 at the Structures Laboratory of the “Pontificia Universidad Católica del Perú” to study the interaction between an existing RC frame and a new infill wall built using horizontally-hollow bricks. The cyclic lateral load test proved how the interaction occurred, which ended with mixed failures in the infill wall. The present paper shows two numerical models that try to replicate the load-displacement capacity curve of that cyclic lateral load test: 1) 3D simple micro model using ABAQUS; and 2) seven 2D macro models using ETABS with the equivalent strut method. For both cases, the Concrete Damage Plasticity law was used to simulate the behavior of the concrete elements and the masonry panel. In the macro model, axial stiffness degrading equations dependent on the properties of the equivalent strut were used.

The simple micro model had the best representation of the capacity curve and the plastic deformations followed the cracking pattern of the wall as the experimental test. Regarding the macro model, five gave good results, among them the model in which the width of the equivalent strut is taken as $\frac{1}{4}$ of the diagonal of the masonry panel. This model is also the one adopted by the Peruvian Masonry Code.

KEYWORDS

Infill wall, Concrete Damage Plasticity, Equivalent Strut, Hollow brick, Load-displacement curves

ⁱ Professor, Pontificia Universidad Católica del Perú, Lima, Perú, dquiun@pucp.edu.pe

ⁱⁱ Bachelor's Student, Civil Engineering, Pontificia Universidad Católica del Perú, Lima, Perú qenti.herencia@pucp.pe



INTRODUCTION

Masonry buildings are widely used in Peru and many Latin American countries as a low-cost and practical way to overcome the increasing housing deficit [1]. According to the latest Peruvian National Census of Population and Housing, about 56% of the walls in housing buildings are built with bricks or cement blocks [2]. The economic reasons and the need to have more space in the housing buildings have led to lesser thickness of the masonry walls [3]. The horizontally-hollow bricks (called “pandereta” in Perú) are popularly used in masonry wall constructions. These units are used as non-structural walls for infill reinforced concrete (RC) frames. Although they are not allowed for use in structural walls in seismic areas of Peru, many people use them due to the lack of control, and because they are cheaper than solid bricks. Regarding the use of the infill walls, the experimental research done by Quiun and Sáenz [4] with an RC frame infilled with the “pandereta” bricks, was modelled using two numeric models, in 2D and 3D. The constitutive laws were adapted from Concrete Damage Plasticity (CDP), and the masonry was modeled as the common equivalent diagonal strut, with plastic behavior and degrading stiffness.

MODELING THE FRAME – INFILL WALL INTERACTION

Mechanical parameters for the RC frame and masonry in a 3D model

The initial parameters, such as density, elastic modulus, and Poisson modulus, were defined as the values in Table 1, which also were used in the 2D model.

Table 1: Initial parameters for the 3D and 2D models

Element	Density (ton/mm ³)	Elastic modulus (MPa)	Poisson modulus
Concrete	2.4x10 ⁻⁹	21300	0.15
Masonry	1.35x10 ⁻⁹	2589	0.20

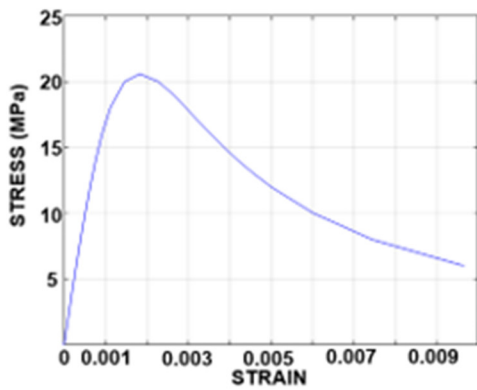
The inelastic behavior of both the concrete of the frame elements and the masonry of the infill wall was done using the Concrete Damage Plasticity (CDP) constitutive model. To achieve this, other values have to be defined, such as the dilatation angle (Ψ) that shows the volumetric expansion of the material in the plastic stage; the eccentricity, that controls the curvature of the yield surface in the modified Drucker-Prager plasticity model; the ratio f_{b0}/f_{c0} , gives the relation between the biaxial compression f_{b0} and the uniaxial compression strength f_{c0} ; the coefficient k controls the contribution of the second invariant deviation stress in the yield function; and the viscosity parameter controls the viscous softening to improve numerical convergence in finite element analysis, as Lee and Fenves [13]. The values recommended by Hafezolghorani, et al [5] were used and are included in Table 2.

Table 2: Inelastic parameters for the 3D model

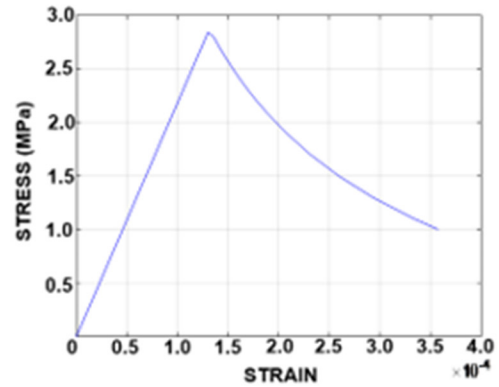
	Dilatation angle (Ψ)	Eccentricity	f_{b0}/f_{c0}	K	Viscosity
Concrete	30	0.1	1.33	0.667	0
Masonry	30	0.1	1.33	0.667	0

The behavior of the concrete in compression and tension is given in Figure 1, with a compressive strength of 21 MPa, and a tensile strength of 2.89 MPa. The behavior of the masonry in compression and tension is given in Figure 2, with a compressive strength of 1.3 MPa, and a tensile strength of 0.7 MPa. The axial

compression test of prisms gave us the value in compression, and the tension value was given somehow arbitrarily to improve the convergence in the model.

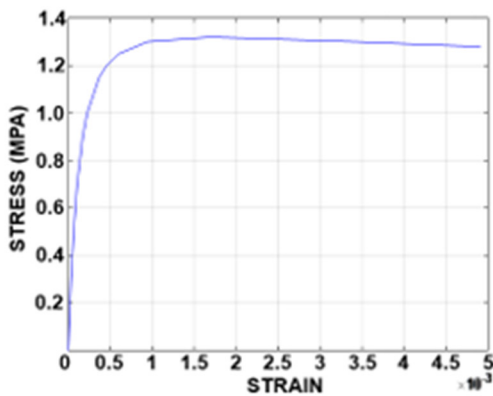


(a) Inelastic compression curve

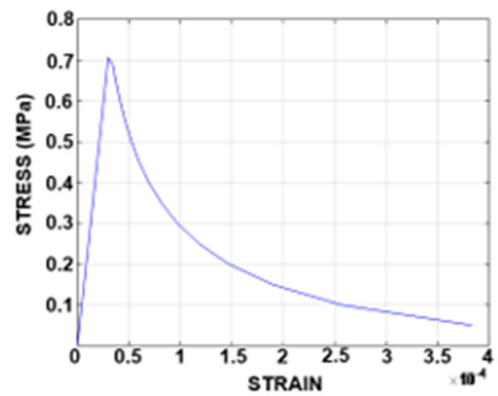


(b) Inelastic tension curve

Figure 1: Inelastic behavior of the concrete in the 3D model



(a) Inelastic compression curve



(b) Inelastic tension curve

Figure 2: Inelastic behavior of the masonry in the 3D model

Mechanical parameters for the reinforcing steel in the 3D model

The mechanical behavior of the reinforcing steel in the frame elements was taken as elastoplastic. The density, elastic modulus, Poisson modulus, and yield stress are given in Table 3. The bars were taken as grade 60 steel.

Table 3: Initial parameters for the Steel in the 3D model

Density (ton/mm ³)	Elastic modulus (MPa)	Poisson modulus	Yield stress (MPa)
7.85×10^{-9}	210,000	0.3	420

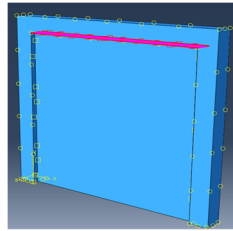
Mechanical parameter for the interface frame – infill wall in the 3D model

The interaction of contact surface-to-surface is simulated as two interfaces where the bodies can transmit normal and tangential forces. The behavior of the tangential forces, cohesion, initial damage, and the interface of the evolution of the damage need to be defined. The tangential behavior deals with the sliding

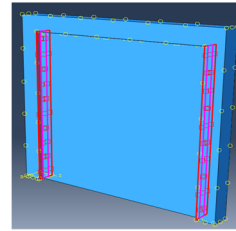
between the contact surfaces. The cohesive behavior determines if the interface has an initial adhesion that can break under the loads. The initial damage indicates if the interface breaks and loses load capacity. The evolution of damage controls how the interface loses stiffness and resistance after the damage begins. Two types of interfaces were defined and analyzed. One interface was used to connect the upper surface of the infill wall and the RC beam, and two interfaces were used to connect the wall lateral borders to the frame columns (Figure 3). The mechanical parameters for the upper interface were taken as those given by Santos et al (2017) [6]. For the lateral interfaces, the mechanical parameters were considered to be equivalent to 60% of the parameters of the upper border. These values are summarized in Table 4.

Table 4: Initial parameters for the interface frame – infill in 3D model

	Tangent behavior		Cohesive behavior (N/mm)			Initial damage (MPa)			Evolution of damage (N-mm)
	Φ	τ_{max} (Mpa)	K_{nn}	K_{ss}	K_{tt}	t_n°	t_s°	t_t°	E_f
Upper Interface	0.5	10.5	5	2,100	2,100	0.91	0.23	0.23	0.05
Lateral Interface	0.3	6.3	3	1,260	1,260	0.55	0.14	0.14	0.03



(a) Upper interface

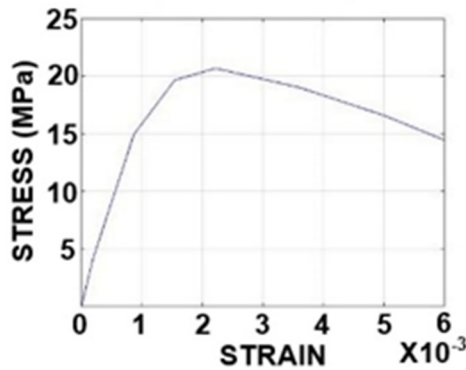


(b) Lateral interface

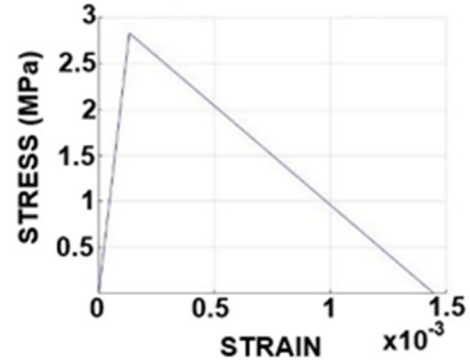
Figure 3: Interfaces in 3D model

Mechanical parameters for the concrete and masonry in the 2D model

The initial parameters, such as density, elastic modulus, and Poisson modulus, for both concrete and masonry, were defined as indicated in Table 1. The compressive strength of the concrete was taken as 20.68 MPa, and the tensile strength as 2.83 MPa. Then, using the equations for the constitutive model of the Concrete Parametric Stress-Strain Curve [9], the curve for the inelastic behavior of the concrete was developed, including compression and tension (Figure 4).



(a) Inelastic behavior in compression



(b) Inelastic behavior in tension

Figure 4: Inelastic curve for the concrete in 2D model

Geometric and mechanical parameters for the infill masonry wall

The geometric dimensions and the mechanical properties for the concrete and the masonry are summarized in Table 5.

Table 5: Infill wall geometry and mechanical parameters for 2D model

Parameters			Units
Wall length	L_m	2,500	mm
Wall height	H_m	2,400	mm
Frame length	L_p	3,000	mm
Frame height	H_p	2,650	mm
Wall diagonal length	D	3,465.5	mm
Wall thickness	t_m	105	mm
Frame thickness	t_p	250	mm
Angle between diagonal and horizontal lines of the wall	θ	0.765	rad
Elastic modulus of the masonry	E_m	2,589	MPa
Shear modulus of the masonry	G_m	1075	MPa
Elastic modulus of the concrete	E_p	21,525	MPa
Moment of inertia of the columns	I_p	325×10^6	mm ⁴
Shear stress in the masonry wall	V_m	0.97	MPa

Table 6: Equivalent strut width and structural behavior of the masonry strut

Author	Strut width (mm)	Point 1		Point 2		Point 3	
		P_{cr} (KN)	d_{cr} (mm)	P_{max} (KN)	d_{max} (mm)	P_{ult} (KN)	d_{ult} (mm)
Peruvian masonry code E.070 (2006)	866.4	217	3.54	272	5.73	174	9.55
Holmes (1961)	1,155.2	217	2.65	272	5.73	174	9.55
Mainstone (1971)	405.9	217	7.67	-	-	174	9.55
Mainstone & Weeks (1974)	400	217	7.57	-	-	174	9.55
Liauw & Kwan (1984)	947	217	3.24	272	5.73	174	9.55
Paulay & Priestley (1992)	866	217	3.54	272	5.73	174	9.55
Durrani & Luo (1994)	830	217	3.70	272	5.73	174	9.55

The equivalent width of the diagonal strut was calculated using different expressions [7] [8]. Also, the important points of the axial force-displacement curve were obtained to consider the strut degradation. Table 6 has the results for three important points: elastic limit, maximum strength capacity, and failure

point [10] [11]. Also, the absolute mean deviation and the standard deviation were calculated compared to the one calculated by the Peruvian Code E.070 [8], which is 0.25 D, giving 222 mm (mean deviation) and 296 mm (standard deviation). The curves of axial force-deformation for each width are given in Figure 5.

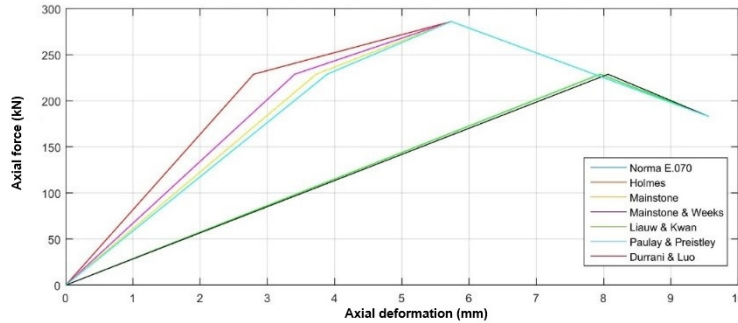


Figure 5: Axial Force-deformation capacity curve for the equivalent strut

Border conditions and load system for the 3D and 2D models

For the 3D model, the bottom base for the concrete frame and the masonry wall were idealized as fully fixed. For the monotonic analysis, in the upper beam, a uniform load was assigned to transmit the displacement amplitudes (Figure 6).



(a) Fixity in the base

(b) Load assignment in the upper beam

Figure 6: Border conditions and load assignment for the 3D model

For the 2D model with the equivalent compression strut, the frame bottom was fixed, as shown in Figure 7 (a). Then, the analysis of the interaction frame-infill was performed using the horizontal load in the upper node, and that way produce displacements into the system, as shown in Figure 7 (b).



(a) Fixity in the base

(b) Load assignment in the upper node

Figure 7: Border conditions and load assignment for 2D model.

EXPERIMENTAL CYCLIC LOAD TEST

The paper by Quiun and Sáenz (2019) [4] shows the experimental program of masonry walls made of horizontally hollow bricks (“pandereta”), a cyclic load test of an infill frame, and an out-of-plane shaking

table test. The lateral cyclic load test was done in an RC frame with masonry infill of such bricks. It consisted of a horizontal displacement-controlled (D1) test in 10 steps, with maximum amplitudes of 1.5, 2, 3, 4, 5, 7.5, 10, 12.5, 15 and 20-mm; all displacements were recorded using LVDTs. Figure 8 shows the horizontally hollow “pandereta” brick used in the infill wall, the structural response of the cyclic-load test, the instruments used as well as the specimen during the testing. The numeric models presented earlier are intended to simulate the results of this cyclic load test.

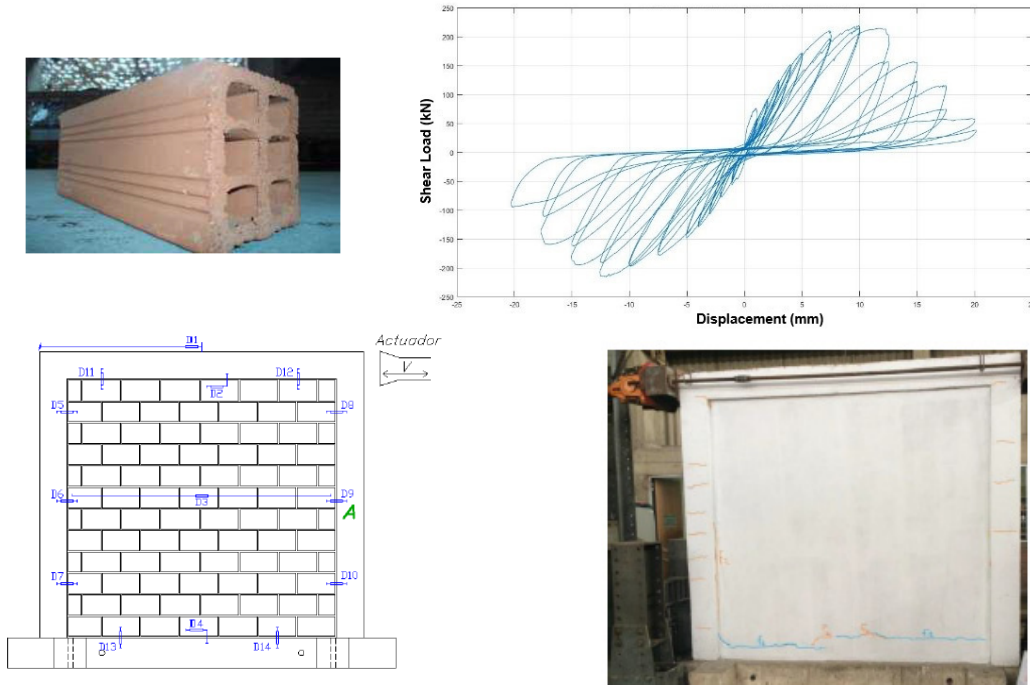


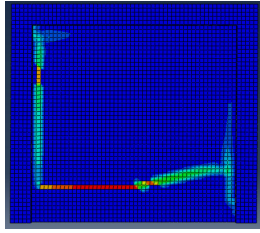
Figure 8: Experimental specimen [4].

NUMERICAL ANALYSIS

The numerical analysis for the 3D model was performed up to a top lateral displacement of 15 mm. The plastic damage is evaluated by a dimensionless parameter that considers the effective plastic strain. Also, in Table 7, a summary of the maximum plastic deformations in the wall (strain PEEQMAX) is given for each step. The material is considered without significant plasticity for the initial maximum displacements of 1.5 mm through 3 mm. Some small plastic deformations appear for displacements of 5 mm and 7.5 mm. Finally, the plastic deformation increased quickly for the maximum displacements of 10 through 15 mm. The frame and infill wall model shows a crack pattern similar to the experimental wall. The final stage of deformations for both the model and the experimental wall is shown in Fig. 9.

Table 7: Maximum plastic deformations in the 3D model

Top displacement	1.5 mm	2 mm	3 mm	5 mm	7.5 mm	10 mm	12.5 mm	15 mm
PEEQMAX	0	7.45×10^{-6}	1×10^{-4}	3.43×10^{-4}	2×10^{-3}	1.7×10^{-2}	2.6×10^{-2}	3.8×10^{-2}



(a) Plastic deformation in 3D model



(b) Crack pattern in the infill wall test

Figure 9: Plastic deformations in 3D model and cracks in the infill wall test

Curve capacity in 3D model

In Figure 10, the load-displacement curve of the numeric 3D model is shown. The maximum shear force reached 213 kN, for a lateral displacement of 7.5 mm, while the experimental value for the same displacement was 219.6 kN.

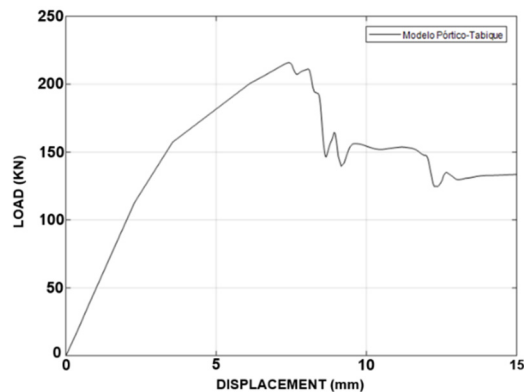


Figure 10: Capacity curve for the 3D model

Comparison of the experimental program vs 3D model and 2D model

The results obtained using the 2D model with the equivalent strut are different as the width of such element varies depending on the proposal equation. If the width is larger, the structural system of the infill frame has greater stiffness but lesser capacity for lateral deformation. The lateral stiffness and the effective stiffness were calculated using the method proposed by Priestley [12].

Table 8 gives a list of these results, and Figure 11 shows the load-displacement capacity curves for all the models and the experimental test curve. It may be noted a good coincidence between the 3D (Abaqus) and the experimental test in the loads (P_{cr} and P_{max}), and stiffness. The 2D models with the equivalent strut give good coincidence with the 3D and the experimental program for the elastic range up to 7.5 mm, which is important if the structural analysis is limited to the elastic behavior.

The stiffness values showed agreement for the models, except in the two expressions of Mainstone and Mainstone & Weeks, in which the stiffness is about half of the other proposed expressions. This significant difference is attributed to the fact that the strut width is the lesser, and in the model, the convergence to the maximum stress was not reached. Therefore, in those two cases, the beginning of yield and maximum load (points 1 and 2, respectively) were taken as the same. The stiffness values obtained by all the other authors have a 9.4% maximum difference with the experimental value. Between the experiment and the 3D model the difference is only 3.7%.

Table 8: Maximum load and displacements comparison in 3D and 2D models

Author	Point 1		Point 2		Lateral stiffness (kN/mm)	
	P_{cr} (kN)	d_{cr} (mm)	P_{max} (kN)	d_{max} (mm)	Initial stiffness (kN/mm)	Effective stiffness (kN/mm)
Quiun & Saenz (Experimental)	76.23	1.5	219.58	7.5	46.9	29.27
Abaqus 3D	85.21	1.71	215.92	7.4	49.57	28.17
Peruvian Masonry Code E.070	173.68	5.4	227.82	8.59	32.16	26.52
Holmes (1961)	172.88	4.2	227.89	8.58	41.16	26.56
Mainstone (1971)	196.87	11.7	196.87	11.7	16.82	16.82
Mainstone & Weeks (1974)	198.40	11.7	198.40	11.7	16.95	16.95
Liauw & Kwan (1984)	177.01	5.1	227.84	8.59	34.70	26.52
Paulay & Priestley (1992)	173.68	5.4	227.82	8.59	32.16	26.51
Durrani & Luo (1994)	176.70	5.7	227.80	8.59	31	26.51

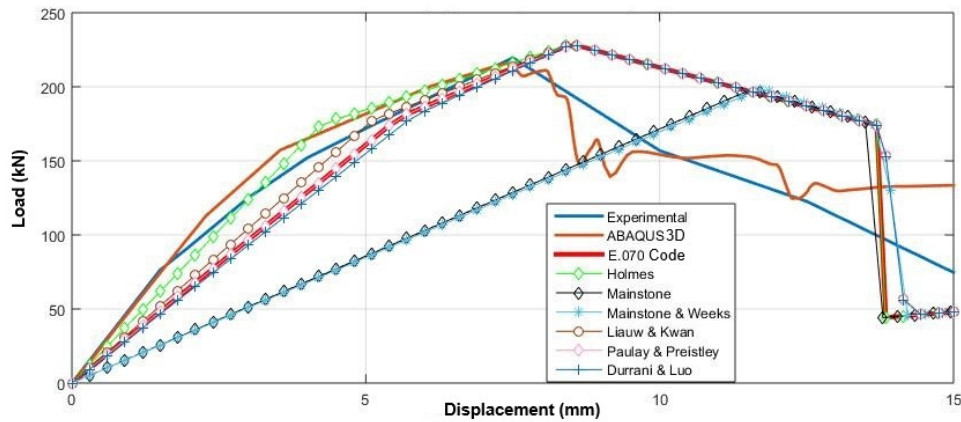


Figure 11: Load-displacement capacity curves for 3D-2D models and experiment

CONCLUSIONS

Using the constitutive law of Concrete Damage Plasticity for both concrete and masonry was very effective because the structural response and system deformation could be simulated. The numerical values for the 3D and 2D models resulted very near to the experimental cyclic lateral load test performed previously by Quiun and Saenz (2019). The 3D model gave results of only 3.7% difference in the lateral effective stiffness and 1.7% difference in the maximum load, and therefore, this 3D model is considered as accurate.

The 2D model adopted by the Peruvian masonry Code E.070 (and many other codes) considers the equivalent strut, in which the equivalent width was calculated with eight different proposed expressions. Although the capacity curves in these 2D models were less precise than the 3D model, the effective stiffness values were quite near, except in the two expressions of Mainstone and Mainstone & Weeks, in which the stiffness is about half of the other proposed expressions. More numerical analyses are needed to understand these differences better. The stiffness values obtained by the other authors gave a maximum 9.4% difference to the experimental value. For design purposes, the strut model can be accepted as good.

ACKNOWLEDGEMENTS

The authors thank professor Cesar Chácara and other structural engineering professors at PUCP for their guidance in the modelling of this research.

REFERENCES

- [1] San Bartolomé, Á., Quiun, D., & Silva, W. (2011). *Diseño y Construcción de Estructuras Sismorresistentes de Albañilería*. Lima: Fondo Editorial de la Pontificia Universidad Católica del Perú.
- [2] Instituto Nacional de Estadística e Informática. (2017). *Censos Nacionales 2017: XII de población, VII de vivienda y III de Comunidades Indígenas*. Lima: Instituto Nacional de Estadística e Informática.
- [3] Pari, S., & Manchego, J. (2017). *Análisis experimental de muros de albañilería confinada en viviendas de baja altura en Lima*. Lima: Tesis de maestría: Pontificia Universidad Católica del Perú.
- [4] Quiun D. & Sáenz, L. (2019). *Experimental seismic behavior of masonry partition walls made of horizontally-hollow bricks*. *Proceedings of the 13th North American Masonry Conference*. Salt Lake City, UT.
- [5] Hafezolghorani, M., Hejazi, F., Vaghei, R., Saleh Bin Jaafar, M., & Karimzade, K. (2017). *Simplified Damage Plasticity Model for Concrete*. *Structural Engineering International*, 68-78.
- [6] Santos, C., Alvarenga, R., Ribeiro, J., Castro, L., Silva, R., Santos, A., & Nalon, G. (2017). *Numerical and experimental evaluation of masonry prisms by finite element method*. *IBRACON STRUCTURES AND MATERIALS JOURNAL*. Vol.10- Nro 2, 477-508.
- [7] AL-Mekhlafy, N., Abdelkareem, K. H., & Abdel Sayed, F. K. (2013). *Equivalent strut width for modeling R.C. infilled frames*. *Engineering Sciences*, 851-866.
- [8] Ministerio de Vivienda Construcción y Saneamiento – SENCICO.(2006).*Norma Técnica de Edificación E.070:Albañilería*. Ministerio de Vivienda Construcción y Saneamiento – SENCICO.
- [9] Computers and Structures, I. (2008). *Technical Note: Material Stress-Strain Curves*.
- [10] Flores, L., & Alcocer, S. (1996). *Calculated response of confined masonry structure*. *Proceedings of the 11th World Conference of Earthquake Engineering* , (pp. 23-28). Acapulco, México.
- [11] Rankawat, N., Brzev, S., Jain, S., & Gavilán Pérez, J. J. (2021). *Nonlinear seismic evaluation of confined masonry structure using equivalent truss model*. *Engineering Structures*.
- [12] Priestley, M. (2000). *Performance-based seismic design*. *XII World Conference on Earthquake Engineering*. Auckland, New Zealand.
- [13] Lee, J., Fenves, G.L. (1998). *Plastic-Damage Model for Cyclic Loading of Concrete Structures*, J. Eng. Mech., 124(8), pp. 892–900, DOI: 10.1061/(asce)0733-9399(1998)124:8(892).